33RD CONGRESS
OF THE INTERNATIONAL COUNCIL
OF THE AERONAUTICAL SCIENCES
STOCKHOLM, SWEDEN, 4-9 SEPTEMBER, 2022

ICAS
2022
SWEDEN

DESIGN OF A TYPICAL MANEUVERING PROCESS SIMULATION TEST CONTROL SYSTEM WITH CONTROLLABLE RUDDER SURFACE

Wang Jianfeng[1], Tan Hao[1], Chen Hao[1],Feng Shuai[1] ,Wang Minghui[1]

[1]AVIC Aerodynamics Research Institute, Heilongjiang Harbin 150001, China

Abstract

In order to simulate the complex maneuvering process of the actual aircraft in wind tunnel environment, we need to implement the decoupling of the respective degrees of the model support system, to realize real-time control of the model rudder surface at the same time.For the wind tunnel test requirements, in this paper, we design the Pitch/Yaw Axis systems controlled by hydraulic drive, the Roll Axis system controlled by servo motor drive, and the Model rudder surface system controlled by the micro-steering gear, realize single-axis high-precision control and multi-axis synchronization control with the method of PID combined with fuzzy control theory in the real-time system, and complete the test system design of typical maneuvering process simulation with the controllable rudder surface. On this basis, we design the typical maneuvering history simulation curves of the Cobra Maneuver, the Tail Thrust Maneuver and the Herbst Maneuver, obtain test data in wind tunnel environment using this test system, verify the system performance by aerodynamic analysis, and prove the reliability of the test system.

Keywords: Maneuvering process; Hydraulic drive; Synchronous control; Wind tunnel test

1. Introduction

Wind tunnel typical maneuvering history simulation test technology (hereinafter referred to as maneuvering history simulation test) is an advanced dynamic test technology with high angle of attack. The discrete data of the maneuvering history of the wind tunnel model are obtained, and the continuous function of the maneuvering history simulation of the wind tunnel scaled model is obtained by smoothing the discrete history data. Aerodynamic force as a function of time [1-4]. The test device is generally realized by single, double, and three degrees of freedom support mechanisms. The model is connected to the support system through the balance. According to the time history curve, the follow-up motion of the model is controlled, and the test history and balance data are recorded at the same time, and then the data analysis work is carried out. The research report on this kind of test technology in foreign countries was earlier. The United States adopted various forms of dynamic test devices developed by it, developed the corresponding wind tunnel typical maneuvering process simulation test technology, and carried out a large number of unsteady aerodynamic characteristics of the maneuvering process for typical layouts. In research work [5-7], NASA Ames Research Center designed an angle-of-attack mechanism driven by a hydraulic servo system in a 10-foot*7-foot wind tunnel, which can achieve rapid maneuvering motion of 0~90° [6], Langley Center is in a 12-foot low-speed wind tunnel, using a hydraulic servo system to drive the angle of attack mechanism to achieve a fast maneuvering motion with a maximum angular velocity of 260°/s and a maximum angular acceleration of 2290°/s^2 in the range of -10~80° [7]. In the DNW-NWB wind tunnel, D&H researchers developed an experimental technique for simulating the motion history of the aircraft over time to obtain the aerodynamic characteristics of the aircraft during the controllable maneuvering of the control surface [8].

A number of domestic universities and research institutes have carried out research work on typical over-stall maneuver simulation tests. Reference [9] used the model-driven field flight test method to carry out the over-stall flight test research of advanced fighter scale models for the first time in China. . Reference [10] established a ground flight simulation environment for man-in-the-loop over-stall maneuvering flight by means of flight simulation. Reference [11] proposed a support method for the Cobra mobile wind tunnel simulation test using tethered parallel structures and verified its feasibility through simulation. The Aerodynamics Research Institute of Aviation Industry has designed a multi-axis decoupling and controllable rudder motion process simulation test system in a wind tunnel environment. The system uses hydraulic and motor drive to design a decoupled model support system. The rudder surface driving mechanism is designed, and the single-axis high-precision control and multi-axis synchronous control are realized through PID combined with fuzzy control theory algorithm under the real-time system. The system is used to complete the simulation of the Cobra maneuvering process, the tail stroke process and the Herbst maneuvering process in the wind tunnel environment. , and obtained experimental data to verify the system performance and reliability.

2. PaperSystem solutions

Taking the test function as the design input, after a given test course, according to the motion parameters contained in the maneuvering action, the simulation of the angle of attack, sideslip angle and rotational motion of the model around the velocity vector is realized by forcing the angle combination of each motion axis of the motion equipment , synchronously manipulate the model rudder surface, and finally realize the model process simulation in the wind tunnel environment. The test system designed in this paper includes the model support system and the rudder surface drive system. The support system also includes the control of the pitch axis degrees of freedom and the roll axis degrees of freedom.

Considering the structural design, the roll axis is installed at the end of the pitch axis mechanism, and the pitch bearing is rotated under the load. The inertia is larger, which requires a larger driving torque. Considering that the hydraulic system has a higher power density than the motor system, in order to reduce wind resistance, the pitch axis is designed with a hydraulic servo system; considering that the roll axis is driven by a hydraulic system, the oil supply pipeline It needs to be transmitted to the end of the roll axis. Due to the continuous motion of the pitch axis relative to the fixed end, the hydraulic pipeline design is more complicated, so the roll axis is designed with a motor servo system; the rudder surface is driven by a micro steering gear, and the system structure is shown in Figure 1.

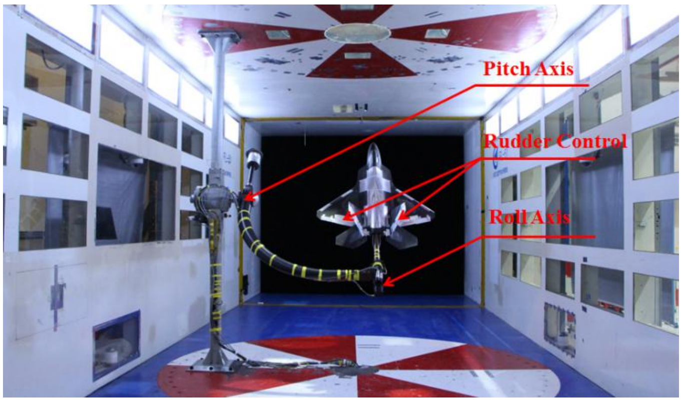

Figure 1 – Simulation test system for maneuvering history

From the above, the design of the maneuvering process simulation test system has been transformed into the design of the hydraulic servo system, the design of the motor servo system, the design of the rudder surface drive system and the synchronous control design of the three, and the simulation of the typical process can be abstracted into the above three. The design of the follow-up control system is introduced separately below.

2.1 Hydraulic Servo System Design

Based on the overall scheme, the pitch axis is driven by hydraulic servo. When a control command is given, the hydraulic motor drives the scimitar to follow the given curve around the center of rotation. In this way, the history simulation movement of pitch or yaw degrees of freedom can be performed. The hydraulic servo drive system is powered by the hydraulic oil source, the hydraulic motor is used as the driving actuator, the flow is adjusted by the opening of the servo valve, and the rotation angle is fed back by the end of the tail support and the motor coaxial encoder [12-14]. The system principle is as follows figure 2.

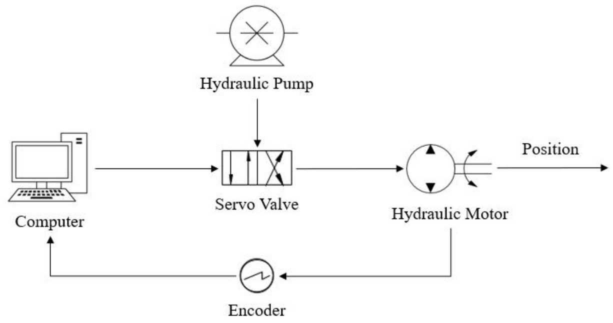

Figure 2 – Schematic diagram of hydraulic servo system

According to the test motion speed and acceleration index, the moment of inertia of the rotating mechanism and load model and other equipment, the key parameters such as motor flow and torque are designed as follows:

Displacement: 450mL/rad

Rated torque: 3200N.m

Servo valve is the core control equipment in hydraulic servo system, and its parameters mainly include rated flow and rated pressure. The design basis depends on the parameters of the matched hydraulic motor to meet the flow required for the maximum angular velocity of the hydraulic motor:

$$q_m = K_l D_m \frac{\dot{\theta}_{\max}}{57.3} \times 60 \tag{1}$$

where:

K_l --- leakage coefficient, dimensionless;

$\dot{\theta}$ ---Maximum angular velocity, unit: $°/s$;

D_m --- Radian displacement, unit: L/rad .

The flow rate that the electro-hydraulic servo valve can provide under the rated pressure is required:

$$q_T = q_m \sqrt{\frac{p_n}{p_s}} \tag{2}$$

where:

q_m ---The required flow rate of the oscillating electro-hydraulic servo motor at the maximum angular speed, unit;

p_n --- Rated pressure of electro-hydraulic servo valve, in MPa;

p_s --- Working pressure of hydraulic oil source, in MPa.

Its calculation results are as follows:

Rated flow: ≥300L/min (7Mpa work)

Select a servo valve with a rated flow of 400 L/min according to the calculated value.

The encoder is used as the feedback element of the hydraulic servo system, and the resolution needs to be more than 5-10 times that of the system control accuracy. In this paper, an incremental encoder with a resolution of 100,000 lines is used. In order to further increase the resolution, the output signal is 4 times. Frequency doubling, the actual resolution is less than 0.1′, which meets the design requirements. Based on the above design of the hydraulic servo drive system, the servo servo control part is introduced in the following chapters.

2.2 Motor Servo System Design

The support rod directly connected to the model shown in Figure 1 is driven by a motor, which can realize the rolling motion of the model. When a control command is given, the motor drives the reducer to realize the harmonic oscillation of the model around the rolling axis or a given curve movement, and the motor servo Compared with the hydraulic servo system, the system has a simple structure and is driven by electricity, including motors, reducers, position feedback components, controllers, etc. [15], as shown in Figure 3.

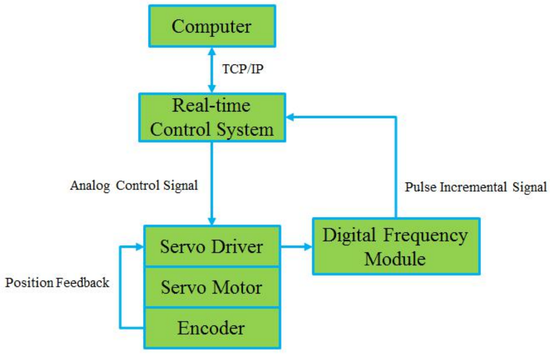

Figure 3 – Composition of motor servo system

The main parameters of motor design include power, torque, etc., which depend on indicators such as struts, model moment of inertia and angular acceleration. Given the 45° /1.2Hz combined harmonic oscillation motion index of the model along the rolling direction, the required parameters such as motor power, speed, torque, and reduction ratio of the reducer are as follows:

Rated power: 0.64Kw

Rated speed: 4050r/min

Rated torque: 1.50N.m

Reduction ratio: 20:1

During the test, the weak current of the force balance signal is transmitted over a long distance. The electromagnetic radiation shielding should be considered in the design of the motor servo system. The drive cable is designed with double shielding, the signal cable is designed with twisted pair shielding transmission, and the grounding of the control system and the grounding of the acquisition system are strict. Distinguish [16-18].

2.3 Rudder drive system design

In the process of simulating the maneuvering process of the aircraft, the model rudder surface moves in real time. For this reason, a micro steering gear and a transmission mechanism are designed to control the rudder surface. In order to reduce the transmission gap, the transmission mechanism is as simple as possible and has a certain strength to prevent damage caused by deformation. Additional error, as shown in Figure 4, the transmission shaft is made of high-quality carbon steel to ensure the rigidity of the rotating shaft, and the self-lubricating bushing ensures the smoothness of rotation, and at the same time ensures the installation of the rudder surface structure.

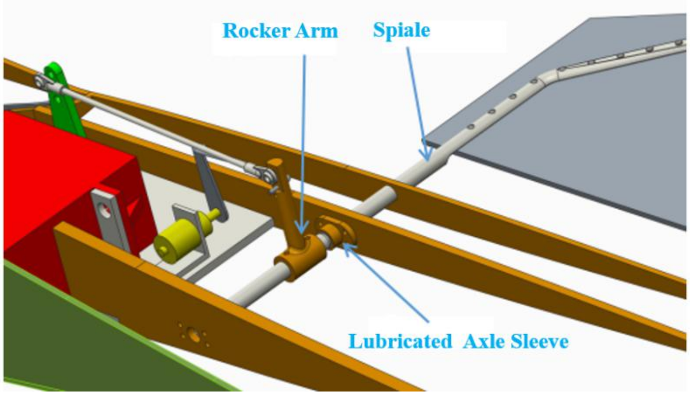

Figure 4 – Servo drive structure

The miniature steering gear integrates the driver and the controller to ensure the size and weight, and adopts the pulse width modulation (PWM) control form [19]. It can be seen from Figure 4 that the rotation angle of the steering surface and the steering gear rotation angle have a nonlinear corresponding relationship, which is Therefore, the rudder surface needs to be corrected, given different duty cycle pulse signals, and the angle measurement tool is used to measure the real-time angle of the rudder surface. Taking the aileron and V tail as examples, the corresponding relationship between pulse signals with different duty ratios (1000us ~ 2000us high level, frequency is 50Hz) and the angle of the rudder surface is shown in Figure 5, from which the angle of the rudder surface is obtained. A polynomial fitting function with a given PWM signal width (the third-order can be used, the fitting effect of higher-order functions is less improved, but the calculation amount will be greatly increased) for the control system. It should be emphasized that, as can be seen from the figure, when the angle of the rudder surface is greater than 35°, the dead zone phenomenon occurs on the rudder surface, which is caused by the structural limitations of the transmission mechanism and the rudder surface itself, which needs to be considered in the control program. Dead zone limit to avoid overheating and burning of steering gear due to locked rotor.

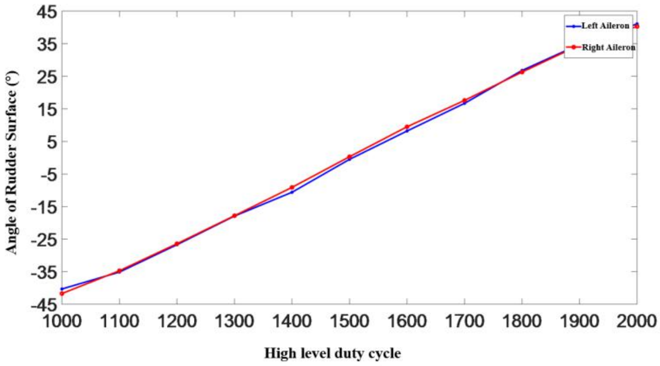

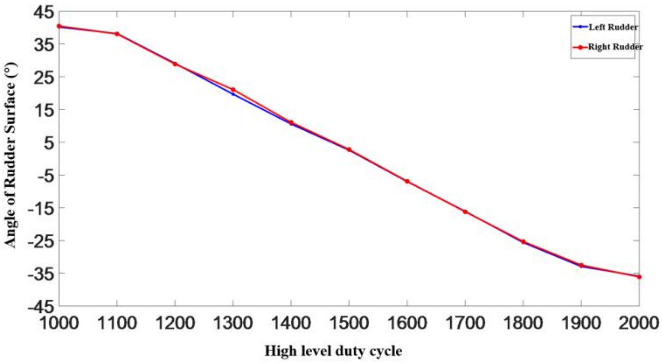

Figure 5 The relationship between the aileron (left) and V tail duty ratio and the angle of the rudder surface

2.4 Synchronous Control and System Implementation

According to the overall scheme of the system, how to achieve high-precision control of each axis and multi-axis synchronous control is the key to the realization of the system. This paper considers from two aspects: firstly, the advanced control algorithm is used to realize the high-precision control of each axis; secondly, the real-time system (program operation) is adopted. Cycle 1ms) as the core of program operation, with high real-time and low delay to ensure the execution efficiency and synchronous control of each axis control algorithm, the control system architecture is shown in Figure 6.

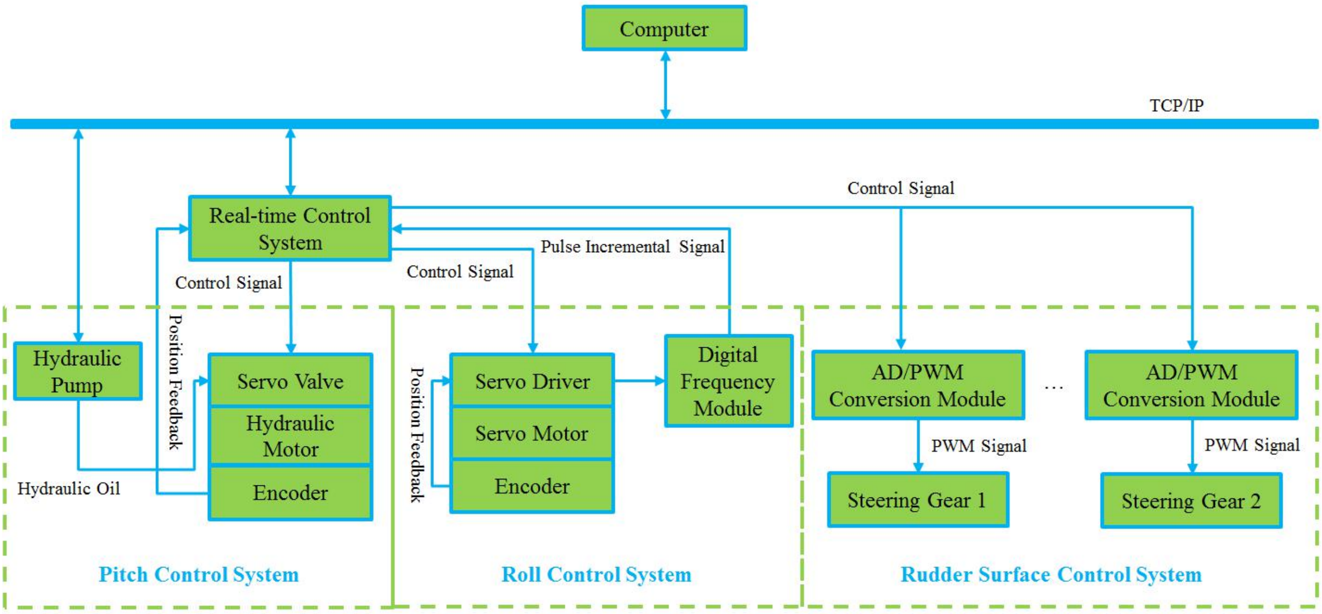

Figure 6 – Control System Architecture

After the test function is modeled, it can be abstracted into a follow-up control system, and the input signal is an arbitrary smooth and derivable continuous curve. The so-called maneuver history simulation even if the system reproduces the follow-up motion of such a given smooth curve, based on this On the above, the synchronous control of time and space is maintained between each axis. Taking the hydraulic servo system as an example, the form of PID+feedforward+fuzzy control is used to realize the high-precision control of the system, as shown in Figure 7. In the specific design of the system index, according to the principle of Fourier transform, the maximum acceleration and speed of the given curve are fitted into a trigonometric function, the frequency index of the trigonometric function is used as the system bandwidth base, and a certain margin is left as the system frequency The input of sound design [20-22].

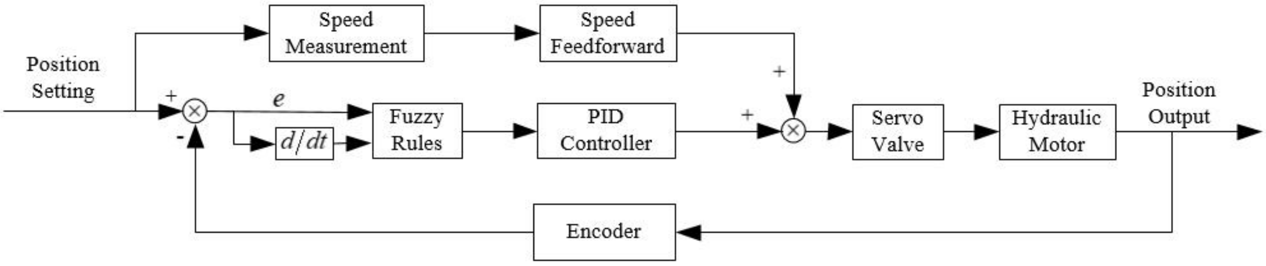

Figure 7 – Overall block diagram of hydraulic servo position control

After the system design is completed, the output response test is carried out with the trigonometric function of the corresponding index as the input condition, as shown in Figure 8, to evaluate the system response in the time domain.

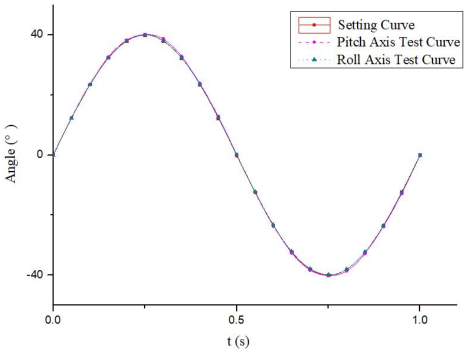

Figure 8 – Pitch axis, roll axis 1Hz/40° index test curve

Figure 9 shows the two-axis position error curve of the synchronous sinusoidal oscillation motion of the hydraulic (pitch) axis and the motor (roll) axis with a 1Hz/40° index. The curve represents the actual motion curve of the two axes and the standard sinusoidal input signal It can be seen that the dynamic error of the pitch axis is less than 0.6° , and the maximum dynamic error of the roll axis is less than 0.3° . Figure 10 shows the synchronous control curves of the pitch axis, roll axis and four rudder surfaces. It can be seen from the figure that each axis has high single-axis control accuracy, good follow-up, and high synchronization signal output and control accuracy, which can meet the needs of typical maneuvering process simulation tests.

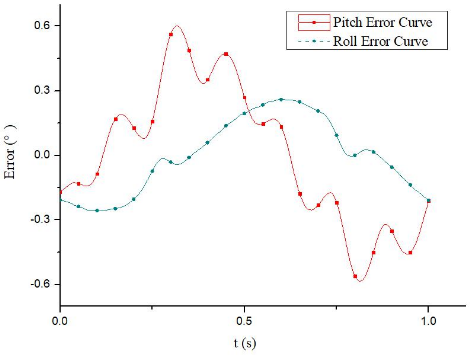

Figure 9 – Index error curve of pitch axis and roll axis 1Hz/40°

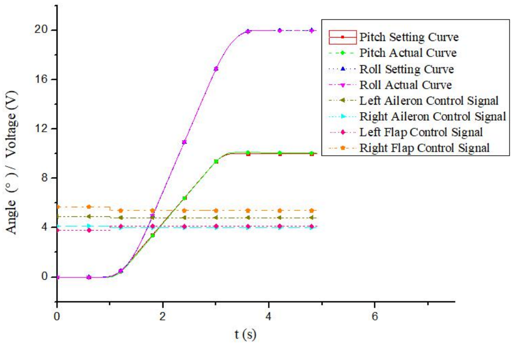

Fig. 10 – Pitch angle, roll angle, and model rudder synchronous control feedback data and error curve

3. Test analysis

3.1 Maneuvering Course Curve Design

Cobra and high angle of attack holding maneuvers are the two most typical high-angle maneuvering flight maneuvers of modern fighter aircraft [23-25]. In order to verify the maneuvering process test system, this paper designs the process for these two maneuvers, including the pitch attitude process. And the motion history of the flat tail rudder surface, the curves are shown in Figures 11-12. The Cobra maneuver starts from the angle of attack in level flight, rapidly increases the angle of attack to 80° in about 1.5 seconds, and then quickly returns to the angle of attack in level flight. The tail thrust maneuver starts from the angle of attack in level flight, rapidly increases the angle of attack to 70° in about 1 second, then maintains a high angle of attack flight state for about 2 seconds, and finally dives quickly.

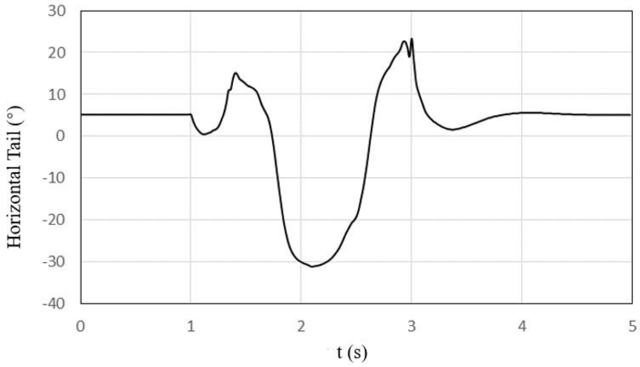

Figure 11 – Cobra maneuver pitch angle and tail course

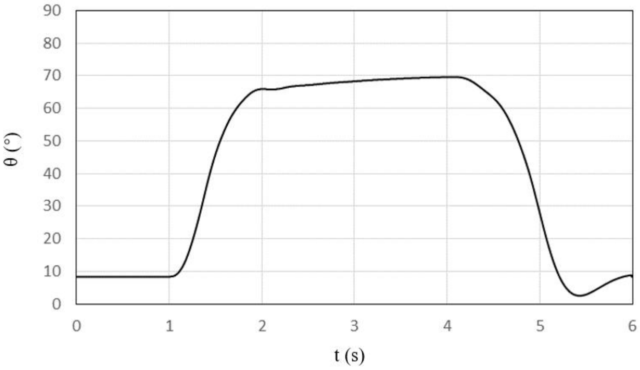

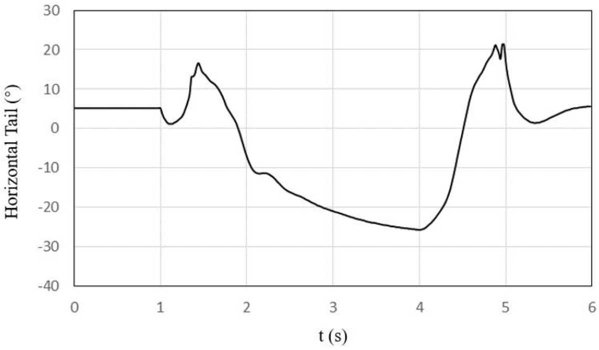

Figure 12 – The process of maintaining the maneuvering pitch angle and the tail at high angle of attack

In addition to the above two longitudinal maneuvers, the Herbst maneuver is a very representative space maneuvering flight action, which can quickly turn to gain tactical advantages in air combat. Aiming at the motion characteristics of the maneuver, this paper also designs the maneuver process simulation. The process of the Herbst maneuver is to raise the angle of attack to about 70° from the level flight state, roll around the velocity vector in the over-stall state, change the nose pointing by 180°, and then reduce the angle of attack to return to the level flight state. In order to simulate this process, the model needs to be back-supported, and the angle between the axis of the model fuselage and the strut is 70°. As shown in Figure 13, in the initial state, the pitch angle of the mechanism is -70°, and the model angle of attack is 0°. Subsequently, the pitch angle of the mechanism was increased to 0°, and the angle of attack of the model was 70°. At this time, the strut was parallel to the direction of the wind speed. After that, the pitch angle of the mechanism remains unchanged, and the 180° rotation around the velocity vector is completed by using the support rod to roll. Finally, the pitch angle of the mechanism is increased to 70°, and the angle of attack is restored to 0°. Figure 14 shows the Herbst maneuver simulation history curve designed according to this principle, excluding the rudder surface movement history, which is used as the input for the verification of the system's synchronous control function.

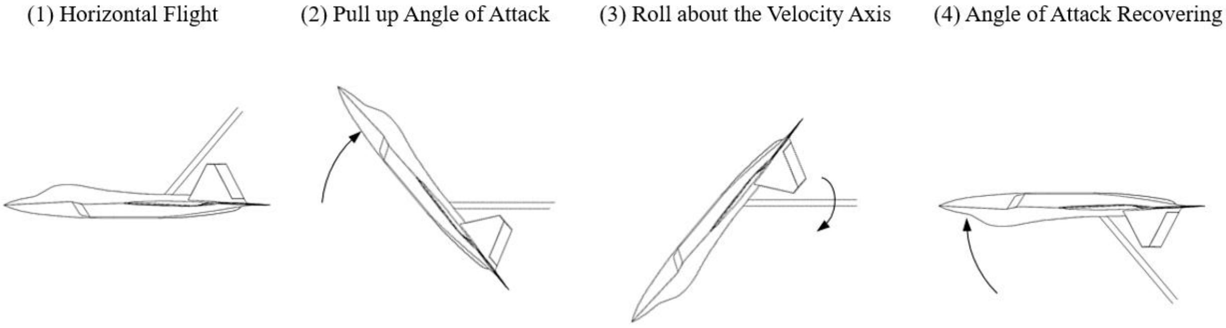

Figure 13 – Design principle of Herbst maneuver simulation process

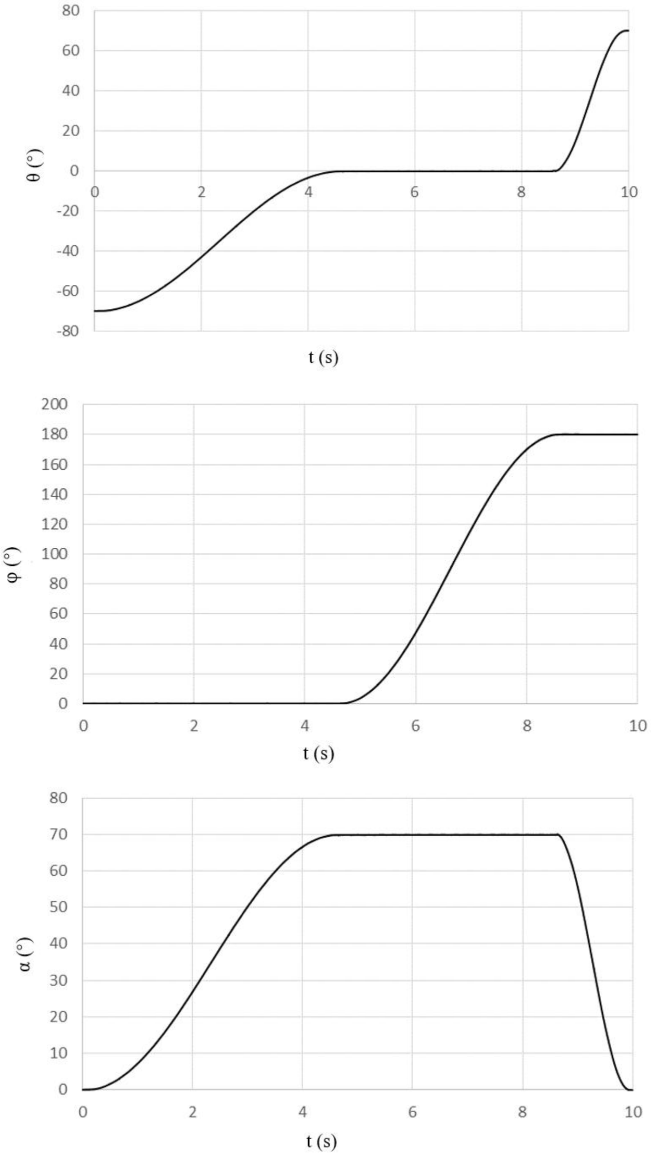

Figure 14 – Herbst maneuver simulation history curve

3.2 Test data analysis

Figure 15, Figure 16, and Figure 17 show the aerodynamic data curves after the balance data collection and processing in the Cobra, high angle of attack hold, and Herbst maneuver history simulation tests, respectively. It can be seen that in the Cobra maneuver, the normal force and the pitching moment form an obvious hysteresis loop curve with the change of the angle of attack. Especially in the large angle of attack range, the area of the hysteresis loop is large, and the hysteresis effect is strong. The overall pitching moment curve presents double "8" characters, indicating that the damping characteristics have changed twice, which fully reflects the nonlinear dynamic characteristics of the model used in the test. The test results of the high angle of attack holding maneuver show the same characteristics as the Cobra maneuver, and the high angle of attack hysteresis is strong. During the Herbst maneuver, the aerodynamic coefficients including the longitudinal and lateral headings also had obvious hysteresis. After the pitch-up, the rotation of the model around the velocity vector had a certain influence on the aerodynamic coefficients, and its influence was significantly weaker than The amount of aerodynamic influence caused by a large change in attitude angle. Therefore, through the wind tunnel test completed by the maneuvering process simulation test system designed in this paper, the force of the aircraft during the maneuvering flight process can be effectively obtained, and the test results are reasonable and credible. The test data obtained through this kind of test can be used for the analysis of the aircraft's high angle of attack and over-stall maneuvering flight characteristics and the verification of the aerodynamic modeling of the aircraft at high angle of attack.

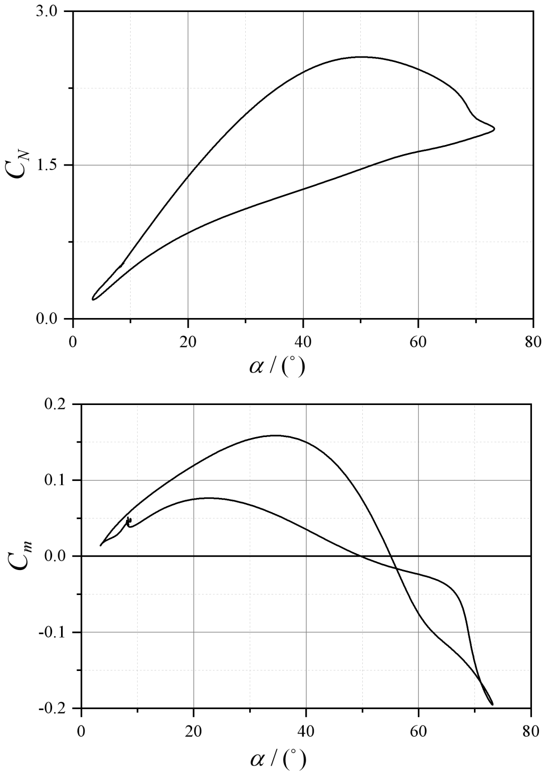

Fig. 15 – Simulation test result curve of Cobra's maneuvering history

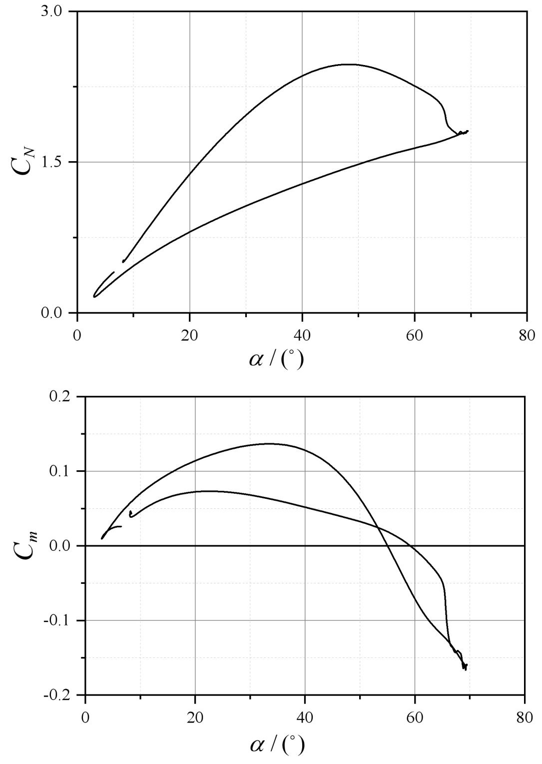

Fig. 16 – The result curve of the simulation test of the high angle of attack maintaining maneuver history

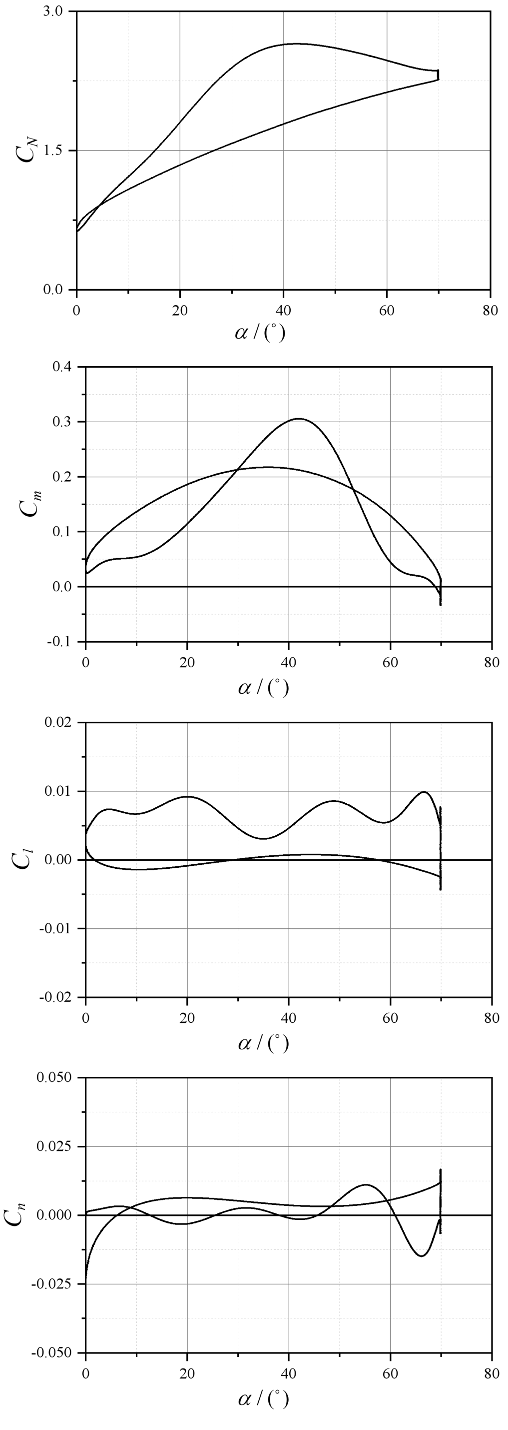

Fig. 17 – The result curve of the Herbst maneuver history simulation test

4. Conclusion

In this paper, a maneuvering process simulation test system with decoupling of pitch axis, roll axis and rudder surface is designed. In the real-time system, the high-precision control and synchronous control of hydraulic servo, motor servo and micro-steering gear can be realized through feedforward and fuzzy PID control algorithm. To meet the test index requirements of the typical maneuvering history curve, by designing the Cobra, tail thrust, and Herbst maneuvering history to simulate the wind tunnel test data analysis, the system can truly reflect the force of the aircraft during the maneuvering flight process, and the test results are reasonable and credible, proving that the The wind tunnel test system can be used for the analysis of the aircraft's high-angle-of-attack and over-stall maneuvering flight characteristics and the verification of the aircraft's high-angle-of-attack aerodynamic modeling.

References

[1] Li Z F. Handbook of Wind Tunnel Test[M]. Beijing: Aviation Industry Press, 2015.

[2] Yang W, Bu C, SUI J J. Unsteady aerodynamic modeling and identification for a complicated aircraft configurations[J]. Acta Aeronautica et Astronautica Sinica, 2016, 37(8): 2464-2471.

[3] Liu C M, Zhao Z J, Bu C, etal. Double degree-of-freedom large amplitude oscillation test technology in low speed wind tunnel[J]. Acta Aeronautica et Astronautica Sinica, 2016, 37(8): 2417-2425.

[4] N.B.Abramov, M.G.Goman, A.N.Khrabrov, K.A.Kolinko. Simple Wings Unsteady Aerodynamics at High Angles of Attack_ Experimental and Modeling Results[R]. AIAA-1999-4013, 1999.

[5] Charles W. Alcorn, Mark A. Croom, Michael S. Francis. The X-31 experience - Aerodynamic impediments to post-stall agility[R]. AIAA-1995-362, 1995.

[6] Mohammad-Ameen M. Jarrah. Low speed wind tunnel investigation of the flow about delta wing, oscillating in pitch to very high angle of attack[R]. AIAA-1989-295, 1989.

[7] Jay M. Brandon, Gautam H. Shah. Unsteady aerodynamic characteristics of a fighter model undergoing large-amplitude pitching motions at high angles of attack[R]. AIAA-1990-309, 1990.

[8] Thomas Loeser, Andreas Bergmann. Development of the Dynamic Wind Tunnel Testing Capabilities at DNW-NWB[R]. AIAA-2003-453, 2003.

[9] HE K F, LIU G, MAO Z J, etal. Model flight test technology for post-stall maneuver of advanced fighter[J]. Acta Aerodynamica Sinica, 2020, 38(1): 9-20.

[10]YANG T J. Flight test driving method of post stall maneuver based on flight simulation [J]. FLIGTH DYNAMICS, 2015, 33(4): 359-363.

[11]Ji Yangfeng. Simulation Research on a Cobra Maneuvering Test Method [J]. Electromechanical Technology, 2020, (6): 2-4.

[12]Wang J F, Bu C, Tan H. Control system design of dynamic test based on hydraulic drive[J]. Acta Aeronautica et Astronautica Sinica, 2017, 38(S1): 721521.

[13]Tang Y D, Liu Y. Electro-hydraulic servo system/ Hydraulic cylinder and systme[M]. Beijing: Chemical Industry Press, 2015.

[14]Liang L H. Hydraulic drive and electro-hydraulic servo system[M]. Harbin: Harbin Engineering University Press, 2005.

[15]Kou B Q, Cheng S K. AC Servo Motor and Control[M] Beijing: Machinery Industry Press, 2008.

[16]He J L. Electromagnetic Compatibility Theory[M]. Beijing: Science Press, 2010.

[17]Sha F. Electromagnetic Compatibility Technology of Mechatronics System[M]. Beijing: China Electric Power Press, 2011.

[18]Yan C, Deng X M, Jia S, etc. A Preliminary Study on Improving EMC Capability for Force Measured Data Acquisition System in Wind Tunnel[J]. Computer Measurement & Control, 2019, 27(9): 28-32.

[19]Sun Y K, Zhang R J, Wu Z G .etc. Dynamic property test and system identification of model aircraft actuators[J]. Journal of Beijing University of Aeronautics and Astronautics, 2020, 46(2):294-303.

[20]Zou W S. Design of a Hydraulic Motor and its Servo System for XX Airborne Radar[D]. Shanghai Jiaotong University, 2014.

[21][Wang M X, Wang H P. Reasearch on the Method of Electro-hydraulic Servo Loading System Based on Adaptive Fuzzy PID Control[J]. Journal of Changchun University, 2013,23(2):130-133.

[22]Zhang Z B, Li S Z, Liu Y J, etc. Design of Hydraulic Cylinder Test Bench Based on Fuzzy PID Control Strategy[J]. Chinese Hydraulics and Pneumatics, 2020,(5):27-32.

[23] Daniel P. R. Post-Stall Maneuver an the classic Turn Rate Plot[R]. AIAA-1915-3170, 1991.

[24]Hong J F. Post Stall Maneuver Simulation Research of Thrust Vector Aircraft and Design of Nonlinear Control Law for High Angle of Attack[D]. Northwestern Polytechnical University, 2003.

[25]Xu Z, Gao H. Mathematical Simulations of Three Typical Post Stall Maneuvers[J]. Flight Dynamics, 1999, 17(3): 11-16.

Copyright Statement